Experimental Neutron Capture Rate Constraint Far from Stability

S. N. Liddick,[1,2] A. Spyrou,[1,3,4] B. P. Crider,[1] F. Naqvi,[1] A. C. Larsen,[5] M. Guttormsen,[5] M. Mumpower,[6,7]
R. Surman,[6] G. Perdikakis,[8,1,4] D. L. Bleuel,[9] A. Couture,[10] L. Crespo Campo,[5] A. C. Dombos,[1,3,4] R. Lewis,[1,2]
S. Mosby,[10] S. Nikas,[8,4] C. J. Prokop,[1,2] T. Renstrom,[5] B. Rubio,[11] S. Siem,[5] and S. J. Quinn[1,3,4]

[1]*National Superconducting Cyclotron Laboratory (NSCL), Michigan State University, East Lansing, Michigan 48824, USA*
[2]*Department of Chemistry, Michigan State University, East Lansing, Michigan 48824, USA*
[3]*Department of Physics and Astronomy, Michigan State University, East Lansing, Michigan 48824, USA*
[4]*Joint Institute for Nuclear Astrophysics, Michigan State University, East Lansing, Michigan 48824, USA*
[5]*Department of Physics, University of Oslo, N-0316 Oslo, Norway*
[6]*Department of Physics, University of Notre Dame, Notre Dame, Indiana 46556, USA*
[7]*Theoretical Division, Los Alamos National Laboratory, Los Alamos, New Mexico 87544, USA*
[8]*Central Michigan University, Mount Pleasant, Michigan 48859, USA*
[9]*Lawrence Livermore National Laboratory, 7000 East Avenue, Livermore, California 94550-9234, USA*
[10]*Los Alamos National Laboratory, Los Alamos, New Mexico 87545, USA*
[11]*IFIC, CSIC-Universidad de Valencia, 46071 Valencia, Spain*

Nuclear reactions where an exotic nucleus captures a neutron are critical for a wide variety of applications, from energy production and national security, to astrophysical processes, and nucleosynthesis. Neutron capture rates are well constrained near stable isotopes where experimental data are available; however, moving far from the valley of stability, uncertainties grow by orders of magnitude. This is due to the complete lack of experimental constraints, as the direct measurement of a neutron-capture reaction on a short-lived nucleus is extremely challenging. Here, we report on the first experimental extraction of a neutron capture reaction rate on ^{69}Ni, a nucleus that is five neutrons away from the last stable isotope of Ni. The implications of this measurement on nucleosynthesis around mass 70 are discussed, and the impact of similar future measurements on the understanding of the origin of the heavy elements in the cosmos is presented.

Neutron capture is the fundamental process by which nearly all of the elements heavier than iron are formed. The abundance pattern of heavy elements from our Solar System shows contributions from two distinct types of neutron capture processes. The slow neutron capture process (*s* process) builds up heavy nuclei slowly, over millions of years, in a sequence of neutron captures that never strays far from stability. The nuclear properties of these mostly stable nuclei, including their neutron capture rates, can typically be measured directly, and as a result, the *s* process has been modeled with precision, although some open questions still remain [1]. The *r* process, on the other hand, involves the rapid capture of neutrons over time scales of the order of seconds or less. Despite decades of speculation, the astrophysical site where the *r* process occurs remains one of the major open questions in science [2]. Many astrophysical environments have been proposed as sites for the *r* process; two of the most favored are supernovae and neutron star mergers, but none seem to explain all of the available data. Further, an increasing body of evidence shows the light (weak, $A \sim 80$–120) *r*-process elements are synthesized separately from the heaviest (main, $A > 120$); thus, two or more sites may be involved [2]. In order to tease out the different contributions from

these two mechanisms in the abundance pattern, significant improvements to *r*-process model inputs are required. The main and weak *r* process are sensitive to nuclear masses, β-decay half-lives, and neutron capture rates. In the main *r* process recent sensitivity studies have demonstrated that these three quantities contribute equally to the uncertainty of the final predicted abundances [3]. While the same type of sensitivity studies have not yet been performed for the weak *r* process, most of the masses and β-decay half-lives are known for the nuclei involved leaving neutron capture rates as the last remaining nuclear physics uncertainty. These neutron capture rates are completely based on theoretical extrapolations from lighter mass systems that introduce large systematic uncertainties.

So far, no experimental pathway exists to determine these neutron capture rates directly on very unstable rare isotopes, as both neutrons and the heavy nuclei of interest are short-lived and thus unsuitable to form a target for accelerator-based experiments. In place of experimental measurements, theoretical calculations are performed within a statistical framework that relies primarily on three separate quantities: the nuclear level density (NLD), γ-ray strength function (γSF), and neutron-nucleus optical model potential. The NLD and γSF are the two nuclear properties

TABLE I. List of models used to describe the NLD and γSF in the Hauser-Feshbach calculations of Fig. 1. Out of the six NLD models available in TALYS, the temperature-dependent Hartree Fock-Bogolyubov level densities using the Gogny force based on Hilaire's combinatorial tables [12] where found during test calculations to produce unphysically strong odd-even effects on the neutron capture reaction rates away from stability. This could be related to systematic disagreements with experimental data mentioned by Hilaire *et al.* in Ref. [12] for odd-odd and odd-*A* nuclei. Furthermore, this model is often not able to reproduce the almost exponential behavior observed experimentally for the level density (see Refs. [12–14]). This possibly unphysical behaviors warrant further investigation and hence the corresponding level density model was deemed not suitable for the sensitivity study of this work. Out of the five available γSF parametrizations, the Brink-Axel single Lorentzian formula [15,16] is known to exhibit a cutoff at lower γ-ray energies at the limit of $E_\gamma \to 0$ that has been shown not to agree with experimental data for neutron capture reactions (see, e.g., Ref. [17]). In general, this model is known to consistently overestimate average and total radiative widths, as well as experimental neutron-capture cross sections for stable nuclei (for example, Refs. [17,18]). Therefore, it was also not used in this work.

Nuclear level density	γ-ray strength function
Constant temperature matched to the Fermi gas model (CT + BSFG) [19]	Kopecky-Uhl generalized Lorentzian (KU) [17]
Back-shifted Fermi gas model (BSFG) [19,20]	Hartree-Fock BCS + QRPA (HF-BCS + QRPA) [21]
Generalized super fluid model (GSM) [22,23]	Hartree-Fock-Bogolyubov + QRPA (HFB + QRPA) [24]
Hartree Fock using Skyrme force (HFS) [25]	Modified Lorentzian (Gor-ML) [26]
Hartree-Fock-Bogoliubov (Skyrme force) + combinatorial method (HFBS − C) [27]	

whose uncertainties have the largest impact on calculated neutron capture rates. The NLD describes the total number of states accessible in a given nucleus at a specific excitation energy. Various methods have been employed to calculate the nuclear level density, which range from a simple Fermi gas model of noninteracting Fermi particles in a common potential to more complex microscopic descriptions [4]. Nuclear level densities have typically been determined for nuclei near stability. In exotic nuclei, such information is completely unknown, and the variation of the nuclear level density as a function of neutron and proton number is uncertain [5]. The γSF defines the average nuclear response to absorbing or emitting a γ ray with a given energy. Together with the NLD, the γSF defines the probability for a nucleus to decay through photon emission after capturing a neutron. The shape of the γSF in exotic nuclei is extrapolated from data for stable nuclei. However, modifications of traditional expectations have been observed even in stable nuclei, as well as some exotic ones. Examples include enhancements in the γSF found close to the neutron separation energy [6] and at very low transition energies [7], which may have a dramatic effect on predicted neutron capture rates [8]. The lack of experimental constraints on the NLD or γSF in exotic isotopes leads to diverging neutron capture rate predictions depending on the choice of NLD or γSF. As a demonstration of this effect, the neutron capture rates for a range of elements from Mn to Ga were calculated using the Hauser-Feshbach statistical reaction code TALYS [9]. The NLD and γSF models given in Table I were varied systematically within the code and the ratio between the largest and smallest neutron capture rate is plotted in Fig. 1. The variations due to differences in the Jekeune-Lejenne-Mahaux [10] Koning-Delaroche [11] optical models was on average 6% for all isotopes considered with the maximum deviation

still under 30%. It is clearly observed in the figure that in moving away from the valley of stability, the variation in the predicted neutron capture rate rapidly increases, with values that reach factors of 20 or more only a few neutrons from the last stable isotope.

To provide experimental constraints on neutron capture rates far from stability, different indirect techniques have been proposed, such as the surrogate reaction technique [28,29] and the γ-ray strength function (γSF) technique [30]. Recently, a new technique was proposed that provides an indirect measurement of neutron capture rates [31] that can be directly applied to short-lived isotopes. The technique is called the β-Oslo method and relies on the measurement of basic nuclear properties (NLD and γSF) that are used as input in (n, γ) reaction calculations. The β-Oslo technique was introduced in Ref. [31] to constrain the neutron capture rate of ^{75}Ge, one neutron less than the stable ^{76}Ge. In the present work, we present the first experimentally constrained (n, γ) reaction rate far from
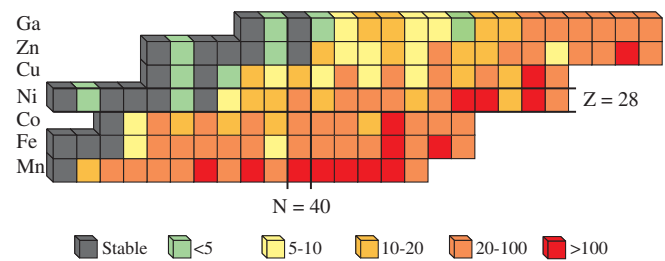

FIG. 1. Ratio of highest to lowest neutron capture rates at 1.5 GK for the isotopes from Mn ($Z = 25$) to Ga ($Z = 31$). The neutron capture rates were calculated with TALYS [9] using the Koning and Delaroche optical model potential [11] and varying the NLD and γSF. The stable isotopes are shown as dark gray squares and all have neutron capture ratios below five.

stability in the mass 70 region, namely, the ^{69}Ni(n, γ) ^{70}Ni reaction, and its impact on astrophysical abundance predictions compared to observational data.

The isotope studied in this work, ^{69}Ni, has five more neutrons than the heaviest stable Ni isotope and has a short half-life (11.4 s), making it unsuitable for direct measurement. The neutron capture on ^{69}Ni into ^{70}Ni was identified in sensitivity studies [32] as influencing the abundances of nuclei produced in weak r-process scenarios. The β decay of ^{70}Co to ^{70}Ni was measured at the National Superconducting Cyclotron Laboratory (NSCL) to infer the neutron capture cross section of ^{69}Ni. A primary beam of ^{86}Kr at 140 MeV/nucleon was reacted with a ^{9}Be target. The resulting fragmentation reaction products were separated in flight using the A1900 fragment separator [33] and delivered to the experimental detector system. The ions were deposited into a 1-mm thick segmented double-sided silicon detector (DSSD) which registered the location and time of arrival of the incoming ions. Each side of the detector had a total of sixteen, 1.2-mm wide strips. Subsequent β decays were also detected and correlated with implanted ions based on time and position information [34]. The correlation technique between ion and β decay was sufficient to remove the contribution of the daughter decay based on the differences in decay half-lives, 105 ms for ^{70}Co and 6 s for ^{70}Ni. The silicon detector was located inside the 45-mm borehole of the Summing NaI (SuN) detector [35]. SuN is a 16 inch $\times$ 16 inch right cylinder of NaI scintillator that is optically segmented into eight separate segments to sum the γ-ray decay energy. SuN has an efficiency of 85% for the 661-keV γ-ray transition from a ^{137}Cs source.

The ground state of ^{70}Co was assumed to have a spin and parity of 6^- based on prior β-decay studies [36] and the allowed decays populate levels in ^{70}Ni leading to levels with spins and parities of 5^-, 6^-, and 7^-. ^{70}Co has a β-decaying isomer with a tentatively assigned spin and parity of 3^+ and a half-life of 0.5 s [36]. This longer-lived β-decaying state strongly populates a known level at 1868 keV with a tentative 2^+ assignment [36–38]. There is no observable peak in the total absorption spectrum at 1868 keV. Further, the time difference between the arrival of a ^{70}Co ion and a subsequent β-decay electron was used to generate the ^{70}Co β-decay curve. The curve was fit with contributions from the exponential decay of ^{70}Co and the growth and decay of the daughter, ^{70}Ni. The half-life of the parent extracted from the fit was consistent with only the short-lived, high-spin, β-decaying state. Allowing for one dipole transition (the primary γ ray) following β decay, daughter levels with spins from 4 to 8 can be populated. The neutron separation energy, S_n, of ^{70}Ni is 7.3 MeV [39].

The β decay of ^{70}Co to ^{70}Ni was measured and the γ-ray cascade following β decay into ^{70}Ni was analyzed using the β-Oslo method [31] which was used to extract the NLD and

γSF of ^{70}Ni. The β-Oslo method differs from the traditional Oslo method only in the mechanism for the population of highly excited states: β decay in the former and light particle reactions in the latter. The NLD and γSF were used to determine the ^{69}Ni$(n, \gamma)^{70}$Ni reaction rate. The NLD and γSF extracted from a traditional Oslo method analysis has a demonstrated ability to reproduce known neutron capture rates in heavier mass nuclei [40].

The β decay of ^{70}Co populated high-energy excited states in ^{70}Ni. SuN provides a measure of both the total photon energy (E_x) emitted following β decay and the individual γ-ray transitions (E_γ) in coincidence with a β-decay electron detected in the DSSD. The γ-ray cascades following the decay of ^{70}Co into ^{70}Ni were analyzed with the following four steps: (i) the unfolding of the detector response from the data for each excitation energy bin [41], (ii) retrieval of the primary γ-ray matrix [42] (the spectrum of the first γ-ray emitted from each excitation energy bin), (iii) extraction of the functional form of the γ-ray transmission coefficient and nuclear level density [43], and (iv) normalization of the two functions [43,44]. The experimentally derived NLD and γSF were normalized to three anchor points [43]: the level density at low excitation energies, the level density near the neutron separation energy, and the average radiative width of levels near the neutron separation energy. The normalization points are taken from available experimental data, systematics, and theoretical calculations.

The NLD was normalized to the low-energy level density and the level density at S_n. The low-energy level density was taken from the experimentally known levels less than a few MeV in excitation energy [37] accounting for the fact that, based on comparisons with neighboring ^{66,68}Ni, it is likely that the discrete level density is incomplete in the region starting around 3 MeV. The combinatorial plus Hartree-Fock-Bogoliubov calculations of Goriely *et al.* [4] were used to constrain the lower and upper values of the level density at S_n. The lower limit of the level density at S_n is 1.02×10^3 MeV^{-1}, leading to an average s-wave neutron resonance spacing, D_0, of 7.43 keV. The upper limit for the level density at S_n is 1.50×10^3 MeV^{-1}, resulting in a D_0 of 4.43 keV. Fermi gas and constant temperature models for the level density were also performed using the phenomenological parameters of von Egidy and Bucurescu [45] and resulted in similar upper limits of $\rho(S_n)$ between 1.3×10^3 and 1.9×10^3 MeV^{-1}. For the present analysis the microscopic calculations were chosen to carry out the normalization. The smaller spin range populated by β decay based on the selection rules of allowed transitions results in reduced lower and upper level-density limits of 5.7×10^2 and 8.4×10^2 MeV^{-1}, respectively. The lower level density was obtained by summing the number of levels with the appropriate spin and parity to be reached by β decay from the microscopic calculation and provided the slope of the
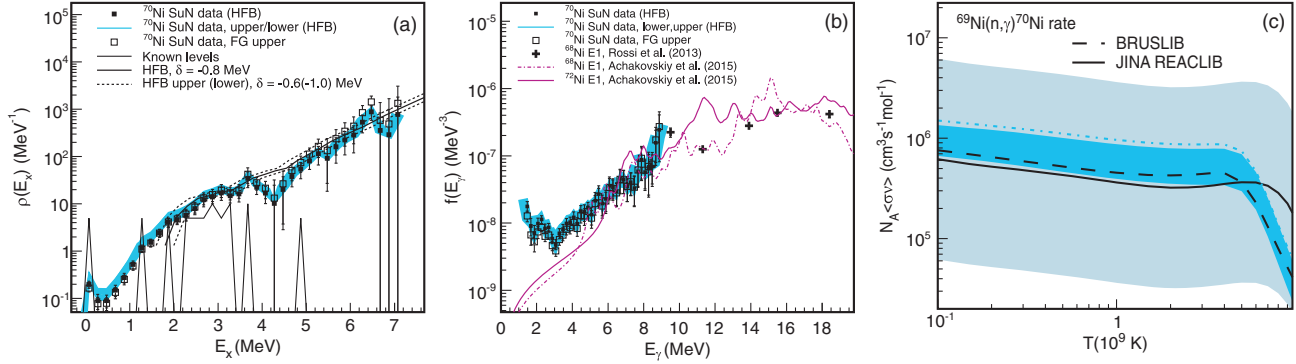
FIG. 2.   (a) Nuclear level density as a function of excitation energy compared to known levels given by the thin black line. High and low experimental bounds using the HFB microscopic normalizations are shown by the blue band. An upper limit from the phenomenological model [45] is provided by the open squares. (b) γSF as a function of γ-ray energy. Experimental data are shown by the black squares with the upper and lower bounds from the microscopic normalization given by the blue band. The experimental data from Rossi *et al.* [46] at higher energies from Coulomb excitation are also shown. The upper bound obtained from the phenomenological model is given by the open squares. Calculations for the $E1$ photon strength of ^{68}Ni and ^{72}Ni [47] are also provided. (c) ^{69}Ni$(n, \gamma)^{70}$Ni reaction rate as a function of temperature. JINA REACLIB [48] and BRUSLIB [49] reaction rate recommendations are shown by solid and dashed lines, respectively. The light-blue shaded band corresponds to a factor of 10 uncertainty in the ^{69}Ni$(n, \gamma)^{70}$Ni reaction rate. The experimental result is provided by the dark blue shaded band. The upper limit using the alternative normalization from Ref. [45] is shown by the blue dot-dashed line.

γSF. The phenomenological models give a similar reduction factor of 47% between the full level density and the level density restricted to states accessible through β decay.

The γSF is normalized to recent Coulomb excitation data on ^{68}Ni [46]. The resulting strength function also matches recent calculations of $E1$ photon strength in neighboring ^{68,72}Ni [47] isotopes. The normalized NLD and γSF are presented in Figs. 2(a) and 2(b).

Using the experimentally normalized NLD and γSF as inputs, the neutron capture rate for ^{69}Ni was calculated using TALYS [9]. The semimicroscopic Jeukenne-Lejeune-Mahaux neutron optical potential was used [9] in the calculations and resulted in the neutron capture rate shown in Fig. 2(c). The reaction rate is compared with the widely used reaction rate libraries BRUSLIB [49] and JINA REACLIB [48]. The ^{69}Ni$(n, \gamma)^{70}$Ni rate is key in low entropy r-process scenarios that produce primarily $A \sim 80$ peak nuclei (weak r process), for example, in the accretion disk outflows that accompany a neutron star [50] or black hole-neutron star merger [51]. To model this environment the weak r process is parametrized with wind conditions similar to previous work [50,51] (entropy $s/k = 10$, time scale $= 0.1$ s, and electron fraction $Y_e = 0.32$). Until the present work, this rate was unconstrained by experiment and the impact of the new rate on this example weak r-process calculation is shown in Fig. 3. A change to this one rate produces a large local shift in abundance from $A = 69$ to 70 (left panel of Fig. 3), and smaller global changes to the abundance pattern ranging up to $A \sim 130$ (right panel of Fig. 3). The uncertainty of the calculations improves dramatically with the new experimental constraints on the ^{69}Ni$(n, \gamma)^{70}$Ni rate. The variations in the

abundance patterns are sharply reduced below 20% everywhere (Fig. 3). Further, by constraining the ^{69}Ni$(n, \gamma)^{70}$Ni neutron capture rate, the uncertainty of the predicted abundances of all mass-70 nuclei now falls below the observation uncertainty for mass-70 nuclei.

The success of this first experimental investigation of a neutron capture rate far from stability paves the path for understanding these important reactions in regions inaccessible until now. The ^{69}Ni$(n, \gamma)^{70}$Ni rate is the first of many key neutron capture rates that can be studied for the
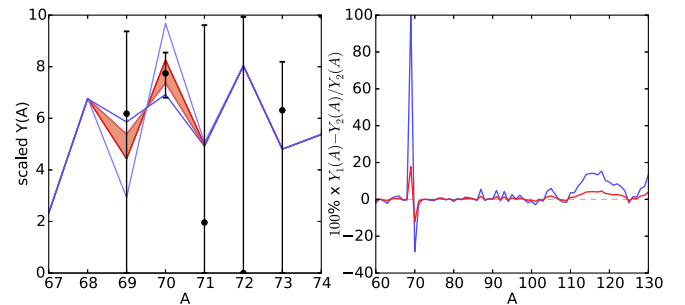

FIG. 3.   (Left) Predicted abundance versus mass number for the weak r process compared to solar r-process residuals (black dots) [2]. The abundance patterns are compared using JINA REACLIB rates with a variation in the ^{69}Ni$(n, \gamma)^{70}$Ni rate of an order of magnitude (blue) and the experimentally constrained reaction rate from the present experiment (red shaded region). (Right) Comparison of the percent abundance change as a function of mass number using old reaction rate uncertainties (blue line) versus the present uncertainties (red). The present data reduce the uncertainties in the abundance predictions to less than 20% across the mass range.
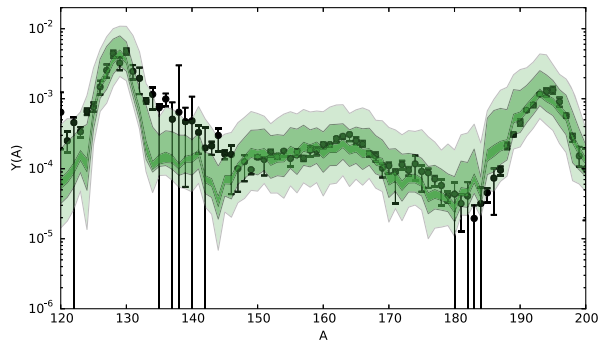
FIG. 4.   Predicted abundances versus mass number compared to solar r-process residuals (black dots) [2]. The shaded bands show the variances in the ensemble of abundance patterns from 20 000 network calculation iterations. In each iteration, a Monte Carlo variation of all neutron capture rates is applied [3]. The shaded bands correspond to neutron capture rate uncertainties of a factor of 100 (light), 10 (middle), and 2 (dark). All but the largest abundance pattern features are obscured by the rate uncertainties at a factor of 100. Only with uncertainties smaller than a factor of 10 can fine features be observed.

weak r process [31]. The main r process, responsible for the $A > 120$ solar residuals, is sensitive to an even larger set of neutron capture rates. The combined effect of all of the present uncertainties on main r-process simulations is illustrated by the light green band in Fig. 4. The main r-process scenario is a neutron star merger trajectory from Bauswein *et al.* [52]. The darker green bands in Fig. 4 represent the predicted abundance uncertainties with increasingly tighter constraints on the variation of the unknown neutron capture rates. The finer details of the abundance features become clearly distinguishable and can be directly compared to the solar residuals only with the smallest level of uncertainty that can be obtained through the application of the present experimental technique on higher-mass nuclei. A systematic program of measurements using the β-Oslo method offers the best hope to reduce neutron capture rate uncertainties to the low level required to differentiate between potential astrophysical r-process scenarios and here we have presented the first step in that direction.

[1] F. Käppeler, R. Gallino, S. Bisterzo, and W. Aoki, Rev. Mod. Phys. **83**, 157 (2011).
[2] M. Arnould, S. Goriely, and K. Takahashi, Phys. Rep. **450**, 97 (2007).
[3] M. Mumpower, R. Surman, G. McLaughlin, and A. Aprahamian, Prog. Part. Nucl. Phys. **86**, 86 (2016).
[4] S. Goriely, S. Hilaire, and A. J. Koning, Phys. Rev. C **78**, 064307 (2008).
[5] S. I. Al-Quraishi, S. M. Grimes, T. N. Massey, and D. A. Resler, Phys. Rev. C **63**, 065803 (2001).
[6] D. Savran, T. Aumann, and A. Zilges, Prog. Part. Nucl. Phys. **70**, 210 (2013).
[7] A. Voinov, E. Algin, U. Agvaanluvsan, T. Belgya, R. Chankova, M. Guttormsen, G. E. Mitchell, J. Rekstad, A. Schiller, and S. Siem, Phys. Rev. Lett. **93**, 142504 (2004).
[8] A. C. Larsen and S. Goriely, Phys. Rev. C **82**, 014318 (2010).
[9] O. Bersillon, F. Gunsing, E. Bauge, R. Jacqmin, and S. Leray, eds., *TALYS-1.6: Proceedings of the International Conference on Nuclear Data for Science and Technology 2007* (EDP Sciences, Nice, France, 2007).
[10] J. P. Jeukenne, A. Lejeune, and C. Mahaux, Phys. Rev. C **15**, 10 (1977).
[11] A. Koning and J. Delaroche, Nucl. Phys. **A713**, 231 (2003).
[12] S. Hilaire, M. Girod, S. Goriely, and A. J. Koning, Phys. Rev. C **86**, 064317 (2012).
[13] A. V. Voinov, B. M. Oginni, S. M. Grimes, C. R. Brune, M. Guttormsen, A. C. Larsen, T. N. Massey, A. Schiller, and S. Siem, Phys. Rev. C **79**, 031301 (2009).
[14] M. Guttormsen, B. Jurado, J. N. Wilson, M. Aiche, L. A. Bernstein, Q. Ducasse, F. Giacoppo, A. Görgen, F. Gunsing, T. W. Hagen, A. C. Larsen, M. Lebois, B. Leniau, T. Renstrøm, S. J. Rose, S. Siem, T. Tornyi, G. M. Tveten, and M. Wiedeking, Phys. Rev. C **88**, 024307 (2013).
[15] D. Brink, Nucl. Phys. **4**, 215 (1957).
[16] P. Axel, Phys. Rev. **126**, 671 (1962).
[17] J. Kopecky and M. Uhl, Phys. Rev. C **41**, 1941 (1990).
[18] R. Capote *et al.*, Nucl. Data Sheets **110**, 3107 (2009), special Issue on Nuclear Reaction Data.
[19] W. Dilg, W. Schantl, H. Vonach, and M. Uhl, Nucl. Phys. **A217**, 269 (1973).
[20] A. Gilbert and A. G. W. Cameron, Can. J. Phys. **43**, 1446 (1965).
[21] S. Goriely and E. Khan, Nucl. Phys. **A706**, 217 (2002).
[22] A. Ignatyuk, K. Istekov, and G. Smirenkin, Sov. J. Nucl. Phys. **29**, 450 (1979).
[23] A. V. Ignatyuk, J. L. Weil, S. Raman, and S. Kahane, Phys. Rev. C **47**, 1504 (1993).
[24] S. Goriely, E. Khan, and M. Samyn, Nucl. Phys. **A739**, 331 (2004).
[25] S. Goriely, F. Tondeur, and J. Pearson, At. Data Nucl. Data Tables **77**, 311 (2001).
[26] S. Goriely, Phys. Lett. B **436**, 10 (1998).
[27] S. Goriely, S. Hilaire, and A. J. Koning, Phys. Rev. C **78**, 064307 (2008).
[28] J. E. Escher, J. T. Burke, F. S. Dietrich, N. D. Scielzo, I. J. Thompson, and W. Younes, Rev. Mod. Phys. **84**, 353 (2012).

[29] J. Cizewski, R. Hatarik, K. Jones, S. Pain, J. Thomas, M. Johnson, D. Bardayan, J. Blackmon, M. Smith, and R. Kozub, Nucl. Instrum. Methods Phys. Res., Sect. B **261,** 938 (2007).

[30] H. Utsunomiya, S. Goriely, H. Akimune, H. Harada, F. Kitatani, S. Goko, H. Toyokawa, K. Yamada, T. Kondo, O. Itoh, M. Kamata, T. Yamagata, Y.-W. Lui, I. Daoutidis, D. P. Arteaga, S. Hilaire, and A. J. Koning, Phys. Rev. C **82,** 064610 (2010).

[31] A. Spyrou, S. N. Liddick, A. C. Larsen, M. Guttormsen, K. Cooper, A. C. Dombos, D. J. Morrissey, F. Naqvi, G. Perdikakis, S. J. Quinn, T. Renstrøm, J. A. Rodriguez, A. Simon, C. S. Sumithrarachchi, and R. G. T. Zegers, Phys. Rev. Lett. **113,** 232502 (2014).

[32] R. Surman, M. Mumpower, R. Sinclair, K. L. Jones, W. R. Hix, and G. C. McLaughlin, AIP Adv. **4,** 041008 (2014).

[33] D. J. Morrissey, B. M. Sherrill, M. Steiner, A. Stolz, and I. Wiedenhoever, Nucl. Instrum. Methods Phys. Res., Sect. B **204,** 90 (2003).

[34] J. I. Prisciandaro, A. C. Morton, and P. F. Mantica, Nucl. Instrum. Methods Phys. Res., Sect. A **505,** 140 (2003).

[35] A. Simon et al., Nucl. Instrum. Methods Phys. Res., Sect. A **703,** 16 (2013).

[36] W. F. Mueller et al., Phys. Rev. C **61,** 054308 (2000).

[37] C. J. Chiara et al., Phys. Rev. C **91,** 044309 (2015).

[38] C. J. Prokop et al. (to be published).

[39] M. Wang, G. Audi, A. Wapstra, F. Kondev, M. MacCormick, X. Xu, and B. Pfeiffer, Chin. Phys. C **36,** 1603 (2012).

[40] T. G. Tornyi, M. Guttormsen, T. K. Eriksen, A. Görgen, F. Giacoppo, T. W. Hagen, A. Krasznahorkay, A. C. Larsen, T. Renstrøm, S. J. Rose, S. Siem, and G. M. Tveten, Phys. Rev. C **89,** 044323 (2014).

[41] M. Guttormsen, T. Tveter, L. Bergholt, F. Ingebretsen, and J. Rekstad, Nucl. Instrum. Methods Phys. Res., Sect. A **374,** 371 (1996).

[42] M. Guttormsen, T. Ramsy, and J. Rekstad, Nucl. Instrum. Methods Phys. Res., Sect. A **255,** 518 (1987).

[43] A. Schiller, L. Bergholt, M. Guttormsen, E. Melby, J. Rekstad, and S. Siem, Nucl. Instrum. Methods Phys. Res., Sect. A **447,** 498 (2000).

[44] A. C. Larsen, M. Guttormsen, M. Krtička, E. Běták, A. Bürger, A. Görgen, H. T. Nyhus, J. Rekstad, A. Schiller, S. Siem, H. K. Toft, G. M. Tveten, A. V. Voinov, and K. Wikan, Phys. Rev. C **83,** 034315 (2011).

[45] T. von Egidy and D. Bucurescu, Phys. Rev. C **80,** 054310 (2009).

[46] D. M. Rossi et al., Phys. Rev. Lett. **111,** 242503 (2013).

[47] O. Achakovskiy, A. Avdeenkov, S. Goriely, S. Kamerdzhiev, and S. Krewald, Phys. Rev. C **91,** 034620 (2015).

[48] R. H. Cyburt, A. M. Amthor, R. Ferguson, Z. Meisel, K. Smith, S. Warren, A. Heger, R. D. Hoffman, T. Rauscher, A. Sakharuk, H. Schatz, F. K. Thielemann, and M. Wiescher, Astrophys. J. Suppl. Ser. **189,** 240 (2010).

[49] The Brussels Nuclear Library for Astrophysics Applications, maintained by Institut dAstronomie et dAstrophysique, Universit Libre de Bruxelles (2015).

[50] S. Wanajo, Y. Sekiguchi, N. Nishimura, K. Kiuchi, K. Kyutoku, and M. Shibata, Astrophys. J. Lett. **789,** L39 (2014).

[51] R. Surman, G. C. McLaughlin, M. Ruffert, H.-T. Janka, and W. R. Hix, Astrophys. J. Lett. **679,** L117 (2008).

[52] A. Bauswein, S. Goriely, and H.-T. Janka, Astrophys. J. **773,** 78 (2013).